Mechanisms of flower movement in *Nicotiana attenuata* Torr. ex S. Wats.

Lucas Cortés Llorca

Trabajo fin de master

Título:

Mechanisms of flower movement in *Nicotiana attenuata* Torr. ex S. Wats.

Autor: Lucas Cortés Ll.

Directores: Herminio Boira[1] and Ian T. Baldwin[2]

Supervisor: Sang-Gyu Kim[2]

[1]Departamento de Ecosistemas Agroforestales, Universidad Politécnica de Valencia, Camino de Vera s/n, 07445, Valencia

[2]Department of Molecular Ecology, Max-Planck-Institute for Chemical Ecology, Hans-Knöll-Str. 8, 07743, Jena

A Germán y Pacos

Introduction

Fine-tuning floral events to the environment is crucial for plant fitness. By changing flowering time, patterns of scent emission, nectar secretion, and flower orientation, plants are able to modulate their interactions with pollinators and herbivores, as well as tolerance against abiotic stress (1, 2, 3, 4). *Nicotiana attenuata* (Solanaceae) is a postfire annual species of the *Artemisio tridentatae - Juniperetea osteospermae* plant community of the Great Basin biogeographical region (5). This species has perfect self-compatible flowers that are visited by hummingbirds, bees, and hawkmoths (6). Typically, flowers start to open at 16:00 hours, reach the maximal corolla extension at 20:00 hours and remain opened for the following three days. Considered as an opportunistic outcrosser, recent data obtained using microsatellite markers shows a surprisingly high outcrossing rate of 44% in naturally pollinated capsules (7). Prezigotic mate selection, emission on benzyl acetone (BA) in phase with pollinator activity or changing pollinators as a way to escape from herbivores are just some examples of the complex and subtlety mechanisms that characterize the reproductive biology of this species (8). In its natural habitat *N. attenuata* plants have to cope with UV-B radiation, drought, a numerous herbivore community (*Tupiocoris notatus* , *Empoasca* sp. , *Manduca* sp., *Corimelaena* sp., *Melanoplus sanguinipes*) and also fluctuations in pollinator populations (D. Kessler, personal communication). Having mechanisms to deal with this complex environment can significantly improve plant fitness, namely, maximizing seed set and outcrossing rates.

Plants have evolved the ability to move their organs by creating an axial asymmetric growth or changes in turgor within cells of specialized organs (pulvinus). Since de Marian first studies in 1729 on leaf movements of *Mimosa pudica*, our

knowledge on the physiological and molecular basis of plant movements has notably increased (9). Two of the best well-characterized plant movements are gravitropism and phototropism. According to the starch-statolith hypothesis, the amyloplasts effect plant growth responses to gravity. Similarly, phototropins (PHOT1 and PHOT2) mediiate plant growth responses to light (10). These growth responses have been widely studied in the opening of hypocotyl hook (11, 12). Hypocotyl straightening is caused by a differential growth and it is correlated to an asymmetric distribution of indole-3-acetic acid (IAA) between adaxial and abaxial flanks, as described by the Cholodny-Went theory (13). Nastic movements are essentially different from gravitropism and phototropisms as they do not respond in growth to a directional stimulus. These movements include the sleeping leaf movements of legume species in which cells in the extensor and flexor regions of the pulvinus swell in antiphase or the clasping leaves of the Venus fly trap (*Dionaea muscipula*) in response to mechanical stimulation (14, 15).

Compared to other floral traits, flower orientation has not attracted much attention and the functionality of this movement spans from pollinator partitioning to protection of pollen grains or facilitation of fertilized ovules development (16). The study of the mechanisms that regulate flower movement will ultimately lead to the understanding of its ecological function.

To characterize the flower movement of *N. attenuata*, we analysed a series of time-lapse acquired images from the anthesis day to flower senescence. Subsequently, we focused on the organ that mainly promoted the flower movement, the pedicel. To address whether changes in curvature were consequence of a differential growth between cells of the adaxial and abaxial parts of the pedicel, we measured cell area with histological techniques. Phytohormone analysis revealed the

accumulation patterns of IAA, indole-3-acetamide (IAM) and IAA-alanine (IAA-ala) overtime in opposite flanks of the pedicel. After establishing pedicel growth *in vitro*, we manipulate auxin asymmetric distribution by exogenously applying IAA or blocking auxin transport with 2,3,5-triiodobenzoic acid (TIBA) in different parts of the pedicel.

Material and methods

Nicotiana attenuata cultivation

N. attenuata seeds derived from a 31x inbred generation were germinated as described by Krügel *et al.* (17). Seeds were sterilized for 5 min in a 5 ml aqueous solution containing 0.1 g of dichloroisocyanuric acid (DCCA: Sigma, St. Louis, MO, USA) supplemented with 50 µl of 0.5% (v/v) Tween-20 (Merck, Darmstadt, Germany). Then, seeds were washed 3 times with sterile water prior to incubation for 1 h in a 5 ml sterile liquid smoke (House of Herbs, Inc.; Passaic, New Jersey,USA) solution 50x diluted supplemented with 50 µl of 0.1 M GA3 (Roth, Karlsruhe, Germany). Seeds were gently rinsed 3 times in sterile water and 50 seeds were transferred, using a sterilized Pasteur pipette, to a petri dish containing the germination media Gamborg's B5 (Duchefa, Haarlem, The Netherlands) and 0.6% Plant agar (Duchefa). The plates were sealed with parafilm and transferred to the growth chamber (Percival, Perry, IA) with a 26°C/16h 155 µm s^{-1} m^{-2} light: 24°C/8h dark cycle. Ten-day old *N. attenuata* seedlings were transferred to TEKU pots (Pöppelmann GmbH & Co. KG, Lohne, Germany) and 10 days later seedlings were transplanted to 1 L pots. Plants growth under greenhouse conditions: 26-28ºC and 16 h supplemental light from Master Sun-T PIA 600 W Na lights (Philips, Turnhout, Belgium).

Flower movement analysis

We characterized flower movement using time-lapse imaging. Plants or individual flowers were tracked from the anthesis to flower senescence. Flower angle was determined as relative to the branch of the inflorescence. To measure pedicel curvature and growth, we excised pedicels from donor wild-type plants (WT) and

transferred them to a petri dish (155 mm x 25 mm) containing 0.6% plant agar (Duchefa). Images were taken every two hours and analyzed using ImageJ (National Institutes of Health, http://rsb.info.nih.gov/ij).

Phytohormone analysis

In order to determine phytohormone accumulation patterns, approximately 100 pedicel flanks were collected at 6:00, 8:00, 12:00, 16:00 and 20:00 hours. Adaxial and abaxial flanks were separated using a razorblade and immediately quick-frozen in liquid N_2. To fulfill the required amount of tissue for the analysis, flanks collected in two consecutive days were pooled. Tissue was ground into a fine powder in liquid nitrogen. Extraction was conducted with 1ml ethyl acetate: formic acid (99.5: 0.5) spiked with phytohormone standards: 40ng of 9,10-D_2-9,10- dihydrojasmonic acid (JA), 40 ng of D_4-salicylic acid (SA), 40 ng of D_6-Abscissic acid (ABA), 8 ng of jasmonic acid-[$^{13}C_6$] isoleucine(JA-Ile) and 10 ng of D_5-indole-3-acetic-acid (IAA). Samples were vortexed for 10 min and centrifuged at 14.000 rpm for 20 min at 4ºC. Supernatants were evaporated to dryness under nitrogen flow. Pellets were then resuspended in 50 µL methanol:water (70:30) solution, dissolved using a ultrasonic bath for 10 min and centrifuged at 10.000 rpm for 10 min at 4ºC. Measurements were conducted on a 1260 liquid chromatography (Agilent) coupled to a mass spectrometer (API 500, Applied Biosystems) (18).Data acquisition and processing was performed with Analyst 1.5 software (Applied Biosystems, Carlsbad, US). Phytohormones were quantified using the signal of their corresponding internal standard.

Auxin and auxin transport inhibitor treatments

With the purpose of modifying auxin distribution and transport, we exogenously applied indole-3-acetic acid (IAA) and 2,3,5-triiodobenzoic acid (TIBA) in lanolin paste. Two independent experiments were conducted in which pedicels were treated at different times (6:00 and 14:00 hours). IAA or TIBA were dissolved DMSO (dimethyl sulfoxide) and added to a pre-warmed (50ºC) lanolin paste to a final concentration of 0.1 mg g^{-1} and 3 mg g^{-1} respectively. The paste was manually applied to the pedicel using a toothpick. A 0.01% (v/w) DMSO in lanolin paste was used as control.

Histochemical analysis

To gain further insight in the auxin response we used transgenic lines carryng the DR5, a synthetic auxin promoter, with the *GUS* (β-glucuronidase) gene. GUS expression was examined by incubating whole seedlings in 100 mM sodium phosphate buffer (pH7.0), 0.5 mM $K_3Fe(CN)_6$, 0.5 mM $K_4Fe(CN)_6$, 10 mM EDTA (pH 8.0), 0.1% Triton X-100 and 1 mM 5-bromo-4-chloro-3-indolyl-β-D-glucuronide at 37ºC for 24 h (). Seedlings were dehydrated through a graded ethanol series and stored in 70% ethanol. Stained seedlings were observed using a stereoscope (Axioplan, Zeiss, Germany) equipped with a digital camera (Axiocam MRc5, Zeiss).

Histology

Pedicels were collected at its maximal degree of curvature (12:00 hours). Longitudinal sections of approximately 100 µm across the middle part of the pedicel were obtained using a vibratome (HM60V, Microm). Sections were incubated for 1 min in a 0.1 % fluorescent brightener 28 (Sigma) solution for staining cell walls, washed to remove the excess of dye and immediately mounted in distilled water.

Sections were observed using an inverted fluorescence microscope (Zeiss) set with an excitation filter BP 450-490 nm, beam splitter FT 510 nm and emission BP 515/565 nm equipped with an axiocam MRc5 (Zeiss) camera. Images were analyzed using AxioVision 4.4 software (Zeiss).

Statistical analyses

All statistical analysis were performed with EXCEL (Microsoft corporation, Redmond, Washington, USA) or Sigmaplot 12.0 for verifying the normal distribution of the data and the ANOVA post hoc tests (Tukey).

Results

Characterization of flower movement

Individual flowers were tracked from the day of anthesis to flower senescence. Epinastic curvature of the pedicel started soon after light stimulation at 6:00 hours. As a consequence, flowers changed from an obliquely upwards (26º±5) to a downwards orientation (-100º±4) between 6:00 and 12:00 hours. Upwards movement typically started at 14:00 when flowers were in a pendulous state and the pedicel was at its maximal degree of curvature. Autostraightening of the pedicel resulted in the recovering of the obliquely upwards orientation (26º±6) of flowers (figs. 1 and 2B).

Flower angle measurements were complemented with kinetic analysis of pedicel growth. Excised pedicels showed a continuous growth from 6:00 to 22:00 hours with a length increment of approximately 0.12 mm h^{-1} (fig 2C).

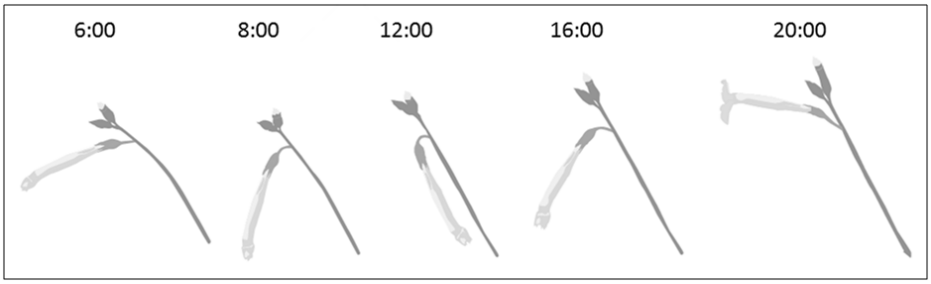

Fig 1. Schematic diagram of *N. attenuata* flower movement

A

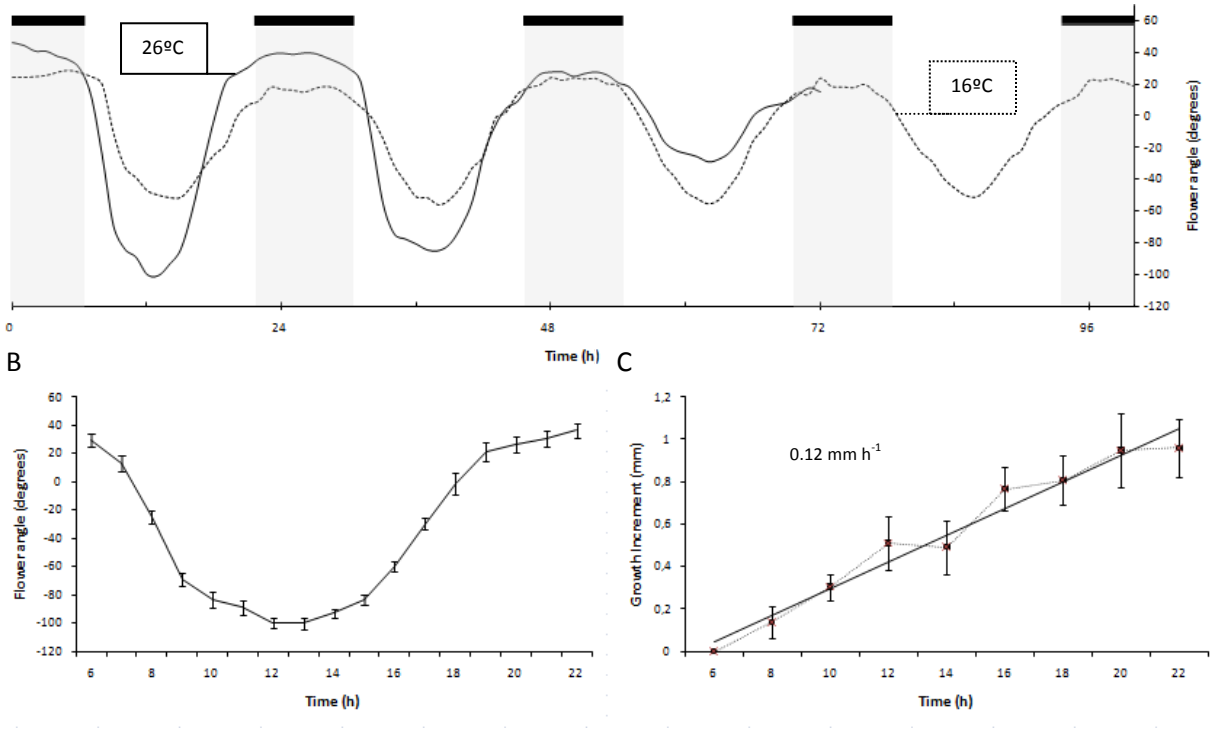

Fig 2. Kinetics of flower angle and pedicel growth. A) Flower angle (mean) from the anthesis to flower senescence at 16ºC and 26ºC (n=6-9). B) Flower angle (mean±SE) on the anthesis day under glasshouse conditions (n=8). C) Pedicel length increment (mean±SE). *In vitro* growth (n=6)

Asymmetric distribution of IAA precedes the development of pedicel curvature

We measured the accumulation patterns of IAA in opposite flanks of the pedicel at 6:00, 8:00, 12:00, 16:00 and 20:00. Initial levels of free IAA didn't significantly differ between both flanks (Fig. 3; t-test, P=0.30). Two hours later, differential accumulation patterns were detected. Auxin levels were significantly higher in the abaxial flank at 8:00, 12:00 and 16:00 (t-test, $p<0.05$). IAA levels increased from 36.93±3.49 to 54.5±4.8 ng g^{-1} between 6:00 and 8:00 hours in the abaxial flank. This increment was found to be correlated in time with the development of epinastic curvature. Opposite flanks didn´t significantly differ in IAA content at 20:00 hours (t-test, P=0.24).

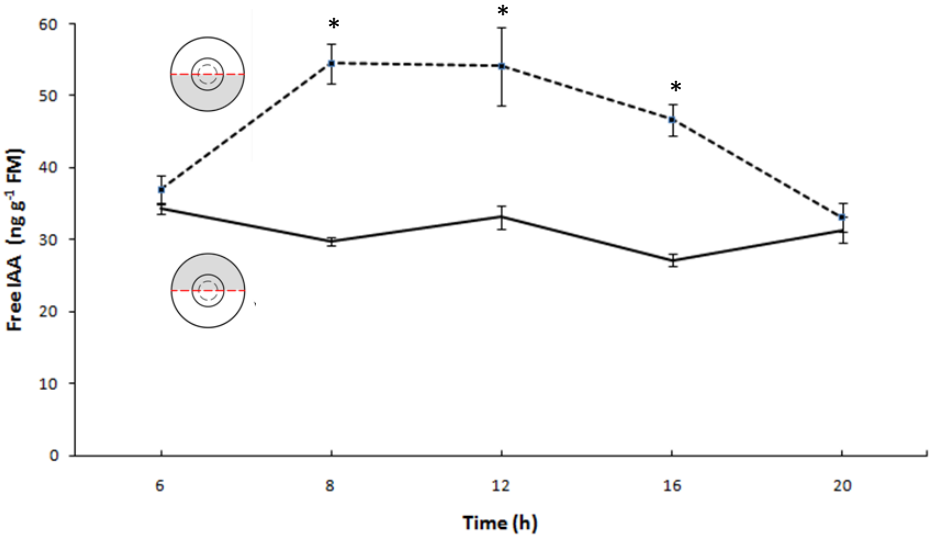

Fig 3. Free IAA levels (mean±SE) in opposite flanks of the pedicel (n=3). Asterisks represent significant differences at $p<0.05$.

Auxins regulate the development of epinastic curvature

To determine the effect of asymmetric distribution of IAA in the development of pedicel curvature, we manipulated endogenous auxin distribution. Equal amounts of TIBA or IAA in lanolin paste were applied to both flanks of the pedicel at 6:00 hours before epinastic curvature started. Initially, flower angle didn't significantly differ from treated and control pedicels at 6:00, 8:00 and 10:00 hours (fig. 4). Curvature development was disrupted in both IAA and TIBA treated pedicels from 12:00 hours. Treated flowers showed significant differences in flower angle at 12:00 and 14:00 hours (t-test, $p<0.05$).

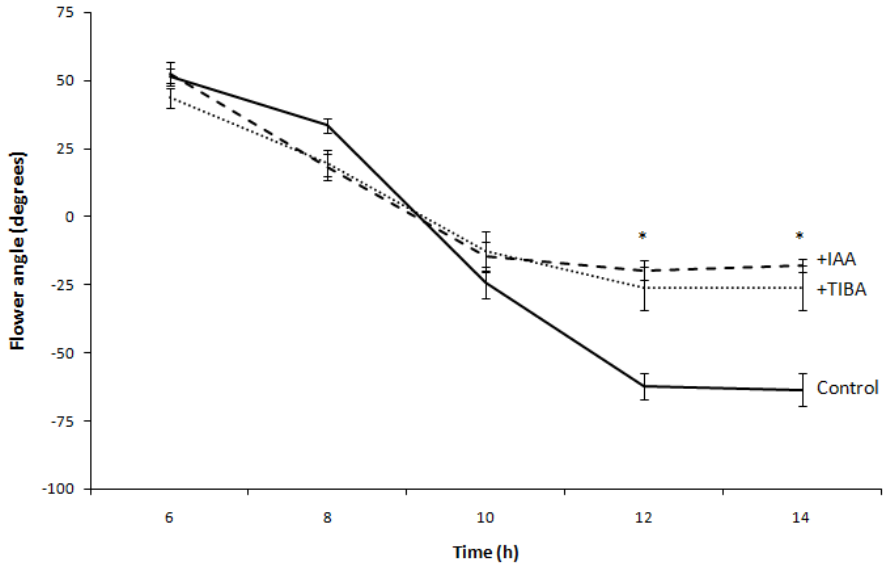

Fig 4. Flower angle (mean±SE) at different time points (n=8). Pedicels were treated with IAA or TIBA in lanolin paste at 6:00 hours. Asterisks represent significant differences at $p<0.05$.

Increase in curvature is correlated with anisotropic cell growth

To address whether the epinastic curvature was correlated with anisotropic cell growth, we measured the size of cells in the abaxial and adaxial flanks of pedicels at their maximal degree curvature (12:00 hours). Cell area was found to be significantly higher in cells of the adaxial flank (fig. 5; t-test, $p<0.05$). Opposite cells showed an approximately 2 fold difference in size.

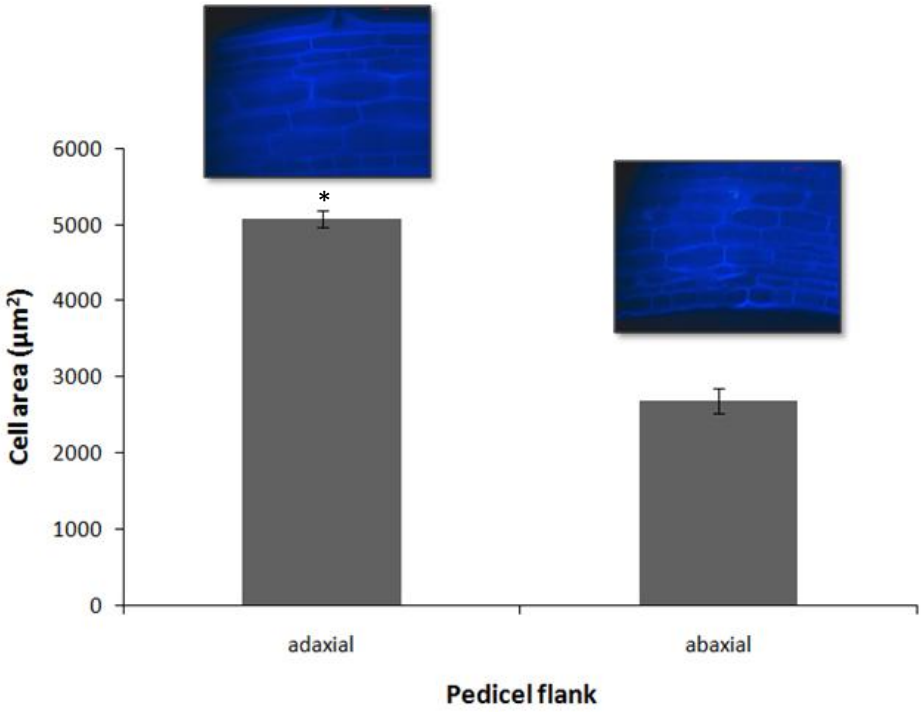

Fig. 5 Area (mean±SE) of individual cells on opposite flanks of the pedicel. Area was measured in pedicels at their maximal degree of curvature (n=50). Asterisks represent significant differences at $p<0.05$

IAA is synthesized in the pedicel

To determine the mechanism that gave rise to the IAA increment in the abaxial part of the pedicel between 6:00 and 8:00 hours we measured the auxin precursor indole-3-acetamide (IAM). IAM levels (relative peak area g^{-1} FM) were significantly higher in the abaxial part of the pedicel at 6:00 hours (fig. 6; t-test, $p<0.05$). IAM levels didn't show significant differences between both flanks at later time points (8:00, 12:00, 16:00 and 20:00 hours).

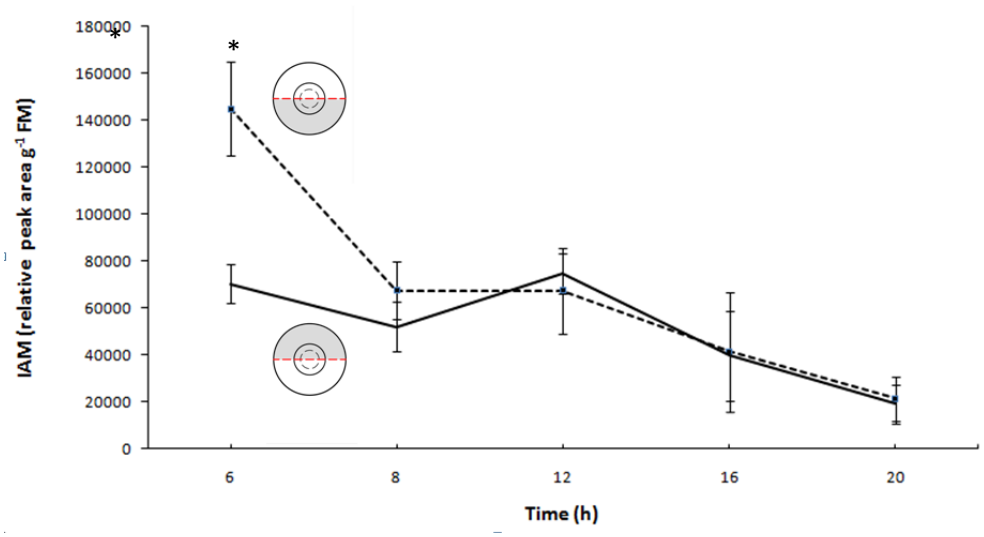

Fig 6. IAM levels (mean±SE) (mean±SE) in opposite flanks of the pedicel (n=3). Asterisks represent significant differences at $p<0.05$.

Auxin conjugates in the pedicel

With the objective to determine the role of IAA conjugates in auxin homeostasis in the pedicel, we measured IAA-Alanine (IAA-Ala), IAA-Isoleucine (IAA-Ile) and IAA-Tryptophan (IAA-Trp). IAA-Ala, IAA-Ile and IAA-Trp levels didn't show significant differences between the adaxial and abaxial parts of the pedicel. IAA-Ile and IAA-Trp levels were close to the limit of detection.

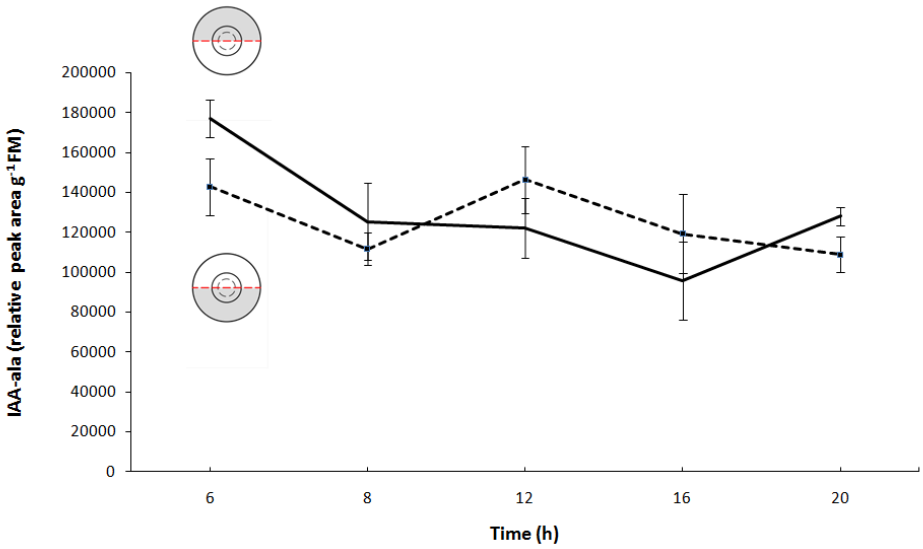

Fig 7. IAA-Ala levels (mean±SE) (mean±SE) in opposite flanks of the pedicel (n=3). Asterisks represent significant differences at $p<0.05$.

Inhibition of auxin transport affects hyponastic straightening of the pedicel

In order to determine the effect of IAA transport on the straightening of the pedicel we applied TIBA in lanolin paste to the abaxial part of the pedicel. TIBA application clearly disrupted flower movement from 18:00. There were significant differences in the angle of TIBA treated flowers at 18:00, 20:00 and 22:00 (fig.8; t-test, $p<0.05$).

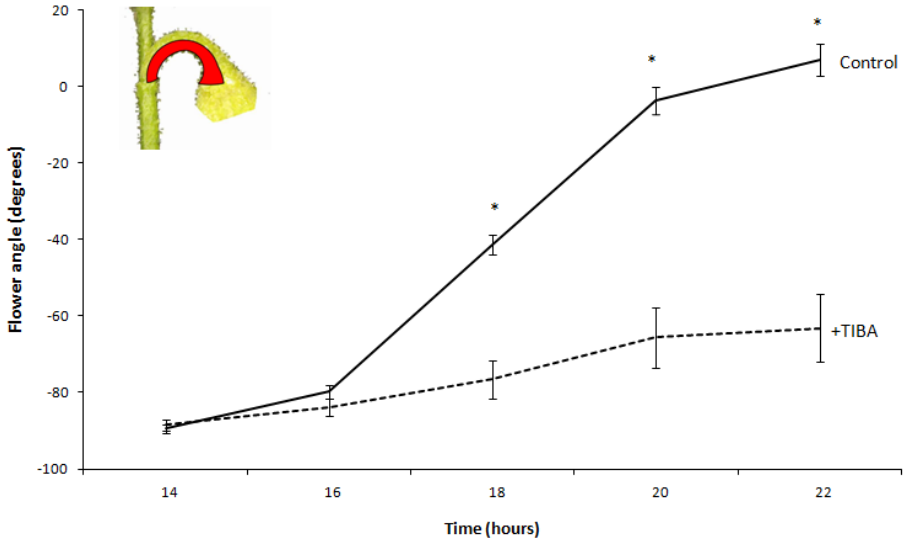

Fig 8. Flower angle (mean±SE) at different time points. Pedicels were treated with TIBA in lanolin paste at 14:00. TIBA was locally applied to the abaxial part of the pedicel (indicated in red). Asterisks represent significant differences at $p<0.05$ (n=7).

To determine the direction of IAA transport, acropetal or basipetal, TIBA was applied to the apical or basal part of the pedicel in two independent experiments. TIBA applied to the base of the pedicel didn´t have significant effect on flower angle. However, when applied to the apical region of the pedicel there were significant differences in flower angle at 16:00, 20:00 and 22:00 hours (fig. 9 B; t-test, $p<0.05$)

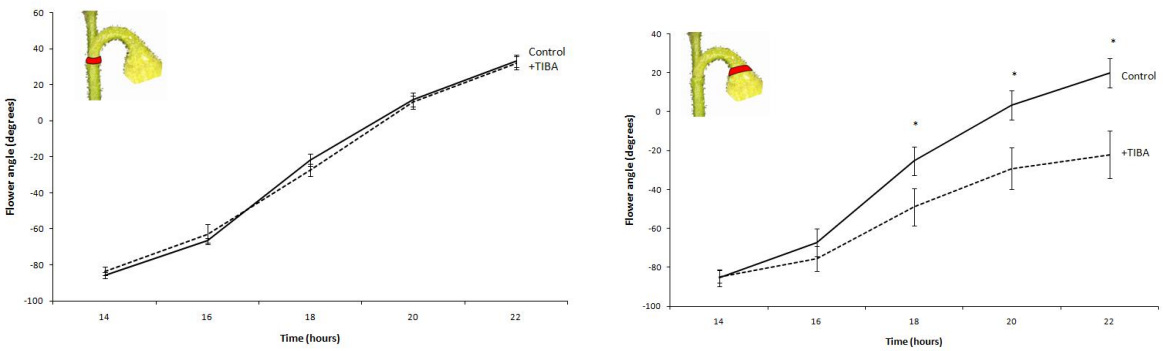

Fig 9. Flower angle (mean±SE) at different time points. Pedicels were treated with TIBA in lanolin paste at 14:00. TIBA was locally applied to the basal or apical regions of the pedicel (indicated in red).. Asterisks represent significant differences at $p<0.05$ (n=7).

Conclusion and future prospects

The studies presented in these pages where initiated in order to characterize the flower movement of *N. attenuata*. We tested the hypothesis that epinastic curvature of the pedicel was a consequence of an IAA asymmetric distribution. We measured the IAA precursor (IAM) and amide-type auxin conjugates to determine the origin of the IAA increment in the abaxial flank of the pedicel. In addition to this, and as a way to find the correlation between auxin asymmetry and pedicel curvature, we modified auxin endogenous levels. Likewise, we measured cell size to determine if this curvature was a consequence of an antiphasic swell or shrinkage of cells in opposite flanks. With the objective of determining the effect of IAA transport in auxin homeostasis in the pedicel, we used an auxin transport inhibitor. And, finally, by blocking IAA transport at specific time points and regions of the pedicel we were able to determine the direction of this transport.

The results obtained support the idea that rhythmic movement of *N. attenuata* flowers is a consequence of an asymmetric distribution of auxins. We found that IAA levels, during epinastic curvature development, are higher in the abaxial part of the pedicel and at the same time cells are bigger in the adaxial flank. These results imply that supraoptimal IAA levels could in fact inhibit cell elongation (19). Furthermore, modifying IAA asymmetric distribution in the pedicel clearly disrupted the movement. This effect is consistent with other growth responses to light and gravity in other species (20). We also found that the increment in IAA levels in the abaxial flank was due to the synthesis of this hormone in the pedicel rather to hydrolysis of amide conjugates or transport from the shoot apical meristem. Blocking auxin transport in the abaxial part of the pedicel before hyponastic straightening disrupted the upwards movement of the flower. This result not only indicates that transport is the main

mechanism for IAA homeostasis but also that a reduction of IAA levels in the abaxial flank is needed for pedicel straightening (21). We further tested the direction of this transport with local applications of TIBA. It was seen that, when applied to the apical part of the pedicel, flowers could not recover an obliquely upwards orientation. IAA transport to the ovary appears to be essential for hyponastic straightening of the pedicel. With the use of the auxin reporter system DR5::GUS we will analyze auxin transport at a future point in time (fig. 9).

We also tested the hypothesis that abcisic acid (ABA) and jasmonic acid-isoleucine (JA-Ile), reported to be involved in other plant movements, could also regulate flower movement in *N. attenuata*. Phytohormone analyses revealed that JA-Ile peak during the hyponastic straightening at 16:00 hours (fig.10). Moreover, plants impaired in JA-Ile perception (irCOI1) didn't show flower movement (fig. 11). These results suggest that JA-Ile could be also involved in the regulation of flower movement probably through a crosstalk with IAA.

Supplemental data

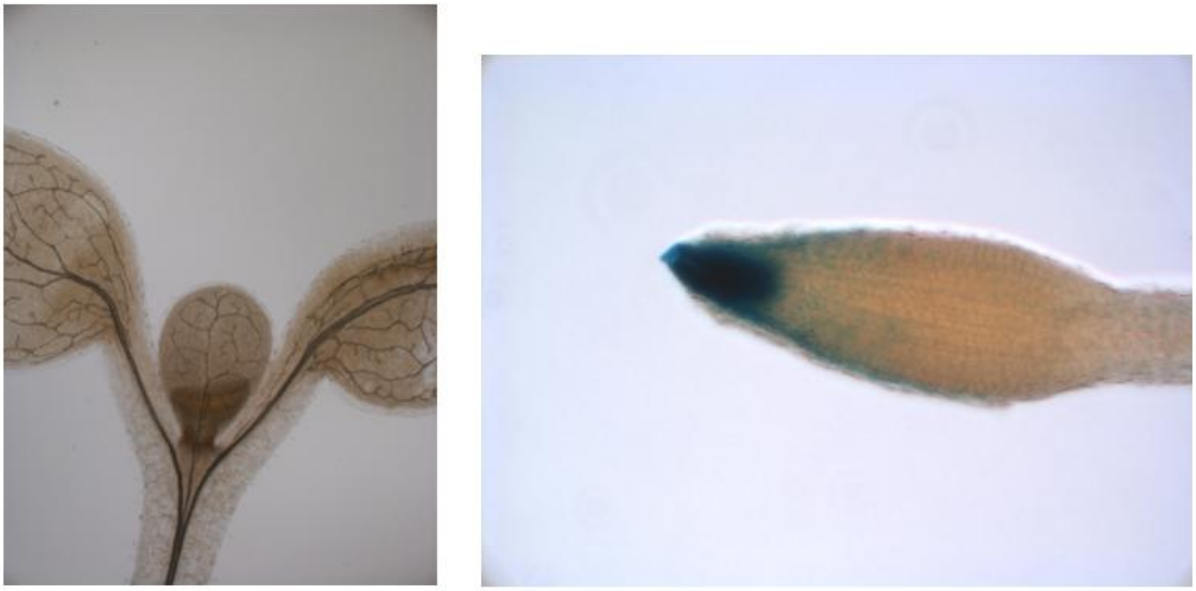

Fig.9 Expression patterns of *DR5::GUS* in *N. attenuata* 10 d seedlings.

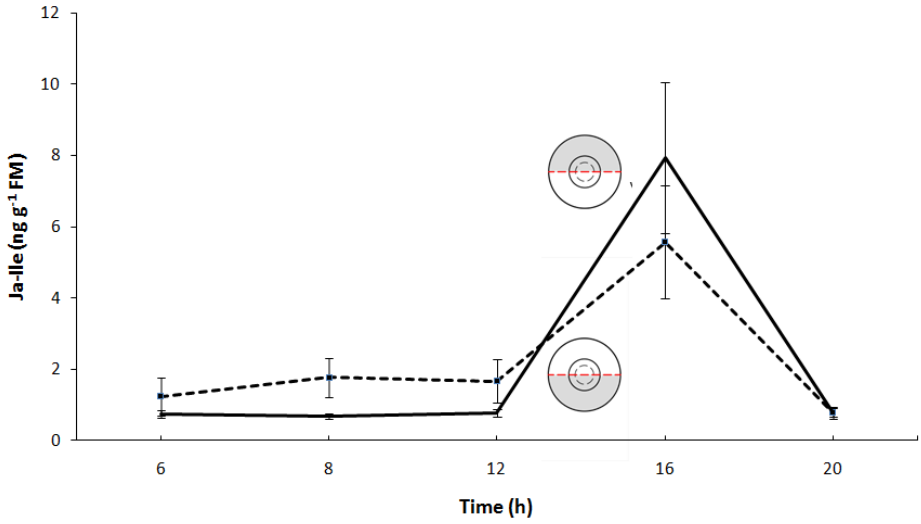

Fig 10. Levels of JA-Ile (mean±SE) in adaxial and abaxial pedicel flanks of wild-type (WT) plants at different times (n=3). Asterisks represent significant differences at ($p<0.05$).

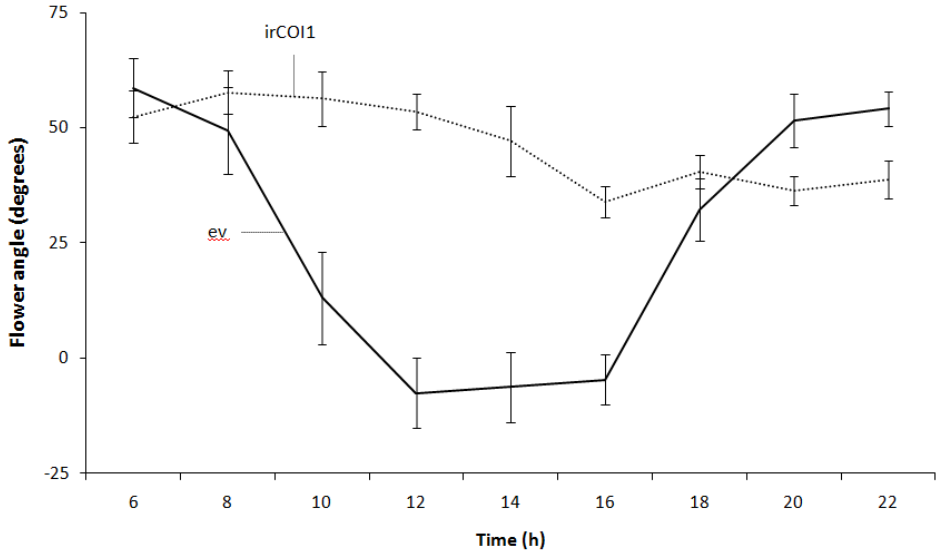

Fig 11. Flower angle (mean±SE) at different time points of empty vector and irCOI1 plants (n=7).

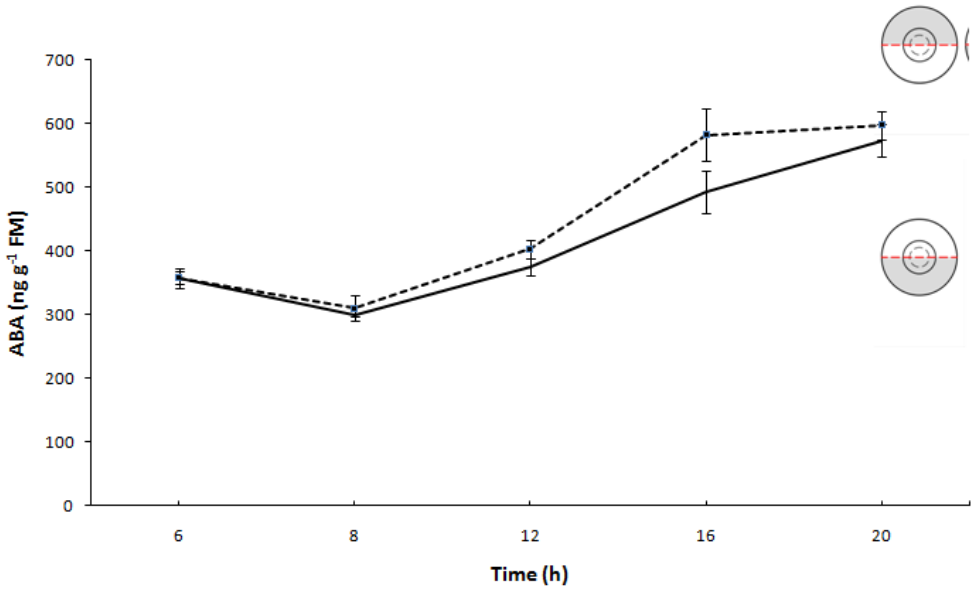

Fig 12. Levels of free ABA (mean±SE) in adaxial and abaxial pedicel flanks of wild-type (WT) plants at different times (n=3). Asterisks represent significant differences at ($p<0.05$).

Acknowledgments

I would like to thank Dr.Sang-Gyu Kim and Professors Ian Baldwin, Herminio Boira and Lleonard Llorens for their help in making this study possible and also, for the scientific discussions shared together.

This study was supported by the ERC-clockworkgreen project and the Max Planck Society.

References

1. Kessler, D., Diezel, C. & Baldwin, I. T. Changing pollinators as a means of escaping herbivores. Current biology 20, 237–42 (2010)

2. Baldwin, I. T., Preston, C., Euler, M. & Gorham, D. Patterns and Consequences of Benzyl Acetone Floral Emissions from Nicotiana attenuata Plants. Journal of Chemical Ecology 23, 2327–2343 (1997)

3. Nepi, M. & Stpiczyńska, M. The complexity of nectar: secretion and resorption dynamically regulate nectar features. Die Naturwissenschaften 95, 177–84 (2008)

4. Eisikowitch, D. & Rotem, R. Flower orientation and color change in *Quisqualis indica* and their possible role in pollinator partitioning. *Botanical Gazette* **148**, 175–179 (1987)

5. Rivas-Martínez, S. Syntaxonomical Synopsis of the potential natural plant communities of North America, I. Itinera Geobotanica 10, 5–148 (1997)

6. Kessler, D. et al. Unpredictability of nectar nicotine promotes outcrossing by hummingbirds in Nicotiana attenuata. The Plant journal 71, 529–38 (2012)

7. Bhattacharya, S., Diezel, C. & Baldwin, I. T. Adaptative mate selection in a native tobacco. Manuscript submitted for publication (2013)

8. Bhattacharya, S. & Baldwin, I. T. The post-pollination ethylene burst and the continuation of floral advertisement are harbingers of non-random mate selection in Nicotiana attenuata. The Plant journal 71, 587–601 (2012)

9. de Marian, M. Observation botanique. Histoire de l'Académie Royale des Sciences 35 (1729)

10. Celaya, R. & Liscum, E. Phototropins and Associated Signaling: Providing the Power of Movement in Higher Plants. Photochemistry and photobiology 81, 73–80 (2005)

11. Watahiki, M. & Yamamoto, K. The massugu1 mutation of Arabidopsis identified with failure of auxin-induced growth curvature of hypocotyl confers auxin insensitivity to hypocotyl and leaf. *Plant physiology* 419–426 (1997)

12. Vandenbussche, F. et al. The auxin influx carriers AUX1 and LAX3 are involved in auxin-ethylene interactions during apical hook development in Arabidopsis thaliana seedlings. Development 137, 597–606 (2010).

13. Thimann, K. V. The cholodny-went “theory”. *Plant Molecular Biology Reporter* **10**, 103–104 (1992).

14. Moran, N. Rhythmic leaf movements: physiological and molecular aspects. *Rhythms in Plants* 3–37 (2007)

15. Volkov, A. G., Adesina, T., Markin, V. S. & Jovanov, E. Kinetics and mechanism of *Dionaea muscipula* trap closing. *Plant physiology* **146**, 694–702 (2008).

16. Wang, Y., Meng, L.-L., Yang, Y.-P. & Duan, Y.-W. Change in floral orientation in *Anisodus luridus* (Solanaceae) protects pollen grains and facilitates development of fertilized ovules. American journal of botany 97, 1618–24 (2010)

17. Krügel, T., Lim, M., Gase, K., Halitschke, R. & Baldwin, I. T. Agrobacterium-mediated transformation of Nicotiana attenuata, a model ecological expression system. *Chemoecology* **12**, 177–183 (2002).

18. Machado, R. *et al.* Roots mediate resource-based trade-offs between shoot regrowth and herbivore defense via jasmonate and auxin signaling. *Manuscript submitted for publication* (2013).

19. Firn, R. & Digby, J. The establishment of tropic curvatures in plants. *Annual Review of Plant Physiology* **31**, 131–148 (1980)

20. Esmon, C. A. *et al.* A gradient of auxin and auxin-dependent transcription precedes tropic growth responses. (2005)

21. Nishimura, T. & Koshiba, T. Auxin Biosynthesis and Polar Auxin Transport During Tropisms in Maize Coleoptiles. *Polar Auxin Transport* 221–238 (2013).doi:10.1007/978-3-642-35299-7